Metrol. Meas. Syst., Vol. 32 (2025) No. 4, pp. 1–17
DOI: 10.24425/mms.2025.155809

METROLOGY AND MEASUREMENT SYSTEMS
Index 330930, ISSN 0860-8229
www.metrology.wat.edu.pl

A MONOCULAR VISION-BASED MOTION PARAMETER MEASUREMENT METHOD FOR LOW-FREQUENCY SHAKERS

Yunpeng Wang[1)], Xiongheng Cao[2)], Hongjiang Chen[2)], Kui Gan[2)], Shanshan Wu[2)], Deguang Wang[1)]

1) Guizhou University, School of Electrical Engineering, Guiyang 550025, China
2) Hunan Institute of Metrology and Test, Changsha 410007, China (✉ *31862083@qq.com*)

Abstract

Accurate measurement of low-frequency vibration parameters is critical for assessing the performance, stability, and dynamic characteristics of mechanical systems. This study proposes a monocular vision-based method for non-contact measurement of motion parameters in low-frequency shakers. The proposed method utilizes high-contrast sinusoidal fringe markers and high-resolution image acquisition to track fringe density variations caused by periodic out-of-plane motion. To enhance frequency estimation accuracy and mitigate spectral leakage, we introduce an improved time-shifting correction method, which features adaptive time-lapse selection and statistical outlier elimination to improve spectral resolution and robustness. Using a calibrated imaging model, the extracted fringe density signals are further processed to derive precise displacement and acceleration values. An experimental platform is established to validate the proposed method against conventional methods based on grating ruler displacement sensors and accelerometers. Experimental results demonstrate that the proposed method achieves high measurement accuracy, with displacement amplitude errors confined within 0.5% and total harmonic distortion values in acceleration measurements below 0.1. Additionally, the proposed method also exhibits excellent stability across a range of low-frequency scenarios. These findings confirm that the proposed method offers a reliable and non-contact alternative for low-frequency vibration measurement, holding strong potential for advancing applications in structural health monitoring, dynamic system diagnostics, and non-destructive testing.

Keywords: monocular vision, low-frequency shakers, vibration measurement, improved time-shifting correction method.

1. Introduction

Vibration measurement technology is an essential element in numerous fields, including industrial manufacturing, structural engineering, aerospace diagnostics, and scientific experimentation [1–4]. Accurate vibration data are critical to evaluating the operational integrity, performance efficiency, and safety of mechanical systems. Traditionally, such measurements have relied on

Article history: received data1; revised data2; accepted data3; available online data4.

contact-based sensors, such as accelerometers and displacement transducers, which convert physical motion into electrical signals for analysis. These sensors offer high sensitivity, mature signal processing techniques, and strong linearity, but face significant challenges in practical applications. Their installation requires precise alignment, secure mounting, and calibration. In addition, they are susceptible to external disturbances, including temperature fluctuations, electromagnetic interference, and mechanical coupling errors. These limitations are particularly pronounced in low-frequency vibration scenarios, where large displacements and slow oscillations reduce the efficacy of traditional sensors, which are typically optimized for high-frequency, small-amplitude conditions [5–7]. Low-frequency signals are also more vulnerable to environmental noise, and their slow temporal changes complicate time-domain analysis. Consequently, there is a pressing need for advanced, high-precision, and non-invasive measurement technologies. Non-contact methods, particularly those leveraging machine vision and optical sensing, have emerged as promising alternatives. These methods eliminate physical contact, minimize measurement-induced disturbances, and offer enhanced flexibility in installation and monitoring. As a result, the development of non-contact vibration measurement methods tailored for low-frequency applications has become a key focus of ongoing research and innovation.

1.1. Brief Review of the Literature

In low-frequency motion scenarios, traditional sensing methods often face significant challenges. Historically, contact-based measurement methods based on laser displacement sensors, accelerometers, and grating rulers have been widely adopted due to their high measurement precision, technological maturity, and broad availability in industrial and research settings [8]. Despite their demonstrated reliability, these conventional methods are constrained by several inherent limitations. Mechanical interference remains a persistent issue, where the physical coupling between the sensor and the structure can inadvertently alter the natural vibration behavior of the system being monitored. In addition, these methods typically involve complex, labor-intensive and invasive installation procedures, which require careful alignment, calibration, and environmental conditioning to ensure measurement accuracy. Moreover, when dealing with high-amplitude and low-frequency vibrations, these sensors often experience performance degradation, struggling to maintain the same level of sensitivity and precision observed at higher frequencies [9–12].

In recent years, non-contact optical measurement methods, particularly those based on machine vision, have emerged as a promising alternative to traditional contact-based vibration measurement methods. By eliminating the need for direct physical attachment to the vibrating body, these methods preserve the natural dynamic behavior of the system while significantly improving the ease of deployment and measurement flexibility. Li *et al.* [13] introduced a machine vision method that estimates the vibration amplitude by analyzing motion blur in sequential images. Tang *et al.* [14] developed a non-contact method aimed at measuring small-amplitude disk vibrations, leveraging camera calibration and coordinate transformation. Dong *et al.* [15] designed a vision-based system capable of multi-point synchronous measurement and modal identification, offering superior adaptability and precision compared to conventional accelerometers. Zhong et al. [16] proposed a tri-axial vibration monitoring system that used sinusoidal fringe patterns of constant-density. Yang *et al.* [17] introduced a monocular vision-based calibration method for low-frequency sensors, incorporating time-spatial synchronization to enhance phase accuracy, which proved particularly effective for frequencies below 0.3 Hz, where it even outperformed laser interferometry. Zuo *et al.* [18] presented an image restoration method to measure low-frequency sinusoidal vibrations. Collectively, these vision-based methods are non-invasive, capable of operating in diverse environmental conditions, and provide high spatial resolution. However, most existing methods

have been optimized for specific operational contexts, typically focusing on medium and low frequency or small-displacement scenarios. As a result, their performance often deteriorates in ultra-low frequency and large amplitude vibration environments, where challenges such as signal instability, low signal-to-noise ratios, and spectral leakage during frequency analysis become more pronounced. To mitigate these issues, researchers have explored various enhancements in signal processing, including the use of window functions and phase-based frequency refinement techniques [19]. Although these strategies yield incremental improvements, they often rely on fixed parameters and remain highly sensitive to noise and signal variability, thus limiting their robustness and effectiveness in real-world and low-frequency measurement applications.

1.2. Our Contributions

Building on the preceding analysis, this study introduces an *improved time-shifting correction method* (ITCM) that significantly enhances frequency estimation accuracy in fringe-based monocular vision systems. By integrating adaptive time-lapse selection with a robust outlier elimination strategy, ITCM effectively addresses persistent challenges of spectral leakage and noise interference, which often compromise the reliability of low-frequency vibration measurements. Furthermore, a new non-contact measurement system is developed to exploit the capability of ITCM. The system utilizes high-contrast and customized fringe markers combined with high-resolution image acquisition, enabling robust capture of low-frequency vibration characteristics with minimal external disturbance or mechanical interference. The main contributions of this study are summarized as follows:

1. ITCM is proposed, which integrates dynamic time-lapse adjustment and statistical outlier suppression. This method significantly improves the accuracy, stability, and robustness of frequency extraction from discrete fringe sequences, particularly in the presence of spectral leakage and noise.
2. A non-contact vibration measurement system is designed, utilizing high-contrast customized fringe markers and high-resolution precision imaging. This system enables reliable, non-invasive, and high-fidelity monitoring of low-frequency vibrational behavior, preserving the natural dynamics of the measured structures.
3. Extensive experimental testing is conducted to benchmark the proposed method against traditional contact-based methods, including grating rulers and acceleration sensors. The results demonstrate that the proposed method achieves high measurement precision in both displacement and acceleration estimations, with superior repeatability and robustness in a wide range of low-frequency vibration scenarios.

The remainder of this study is organized as follows: Section 2 presents the theoretical foundation underlying the proposed methodology. Section 3 describes the system architecture and experimental setup. Finally, Section 4 concludes the study by summarizing the key findings and proposing potential directions for future research and expanded application areas.

2. Methodology

This study introduces an improved methodology to accurately measure the motion parameters of low-frequency shakers using monocular vision. The overall workflow is illustrated in Fig. 1. The process begins with *region of interest* (ROI) identification within captured image sequences. High-contrast fringe markers are isolated to ensure that subsequent analyses focus exclusively on relevant data, enhancing computational efficiency and measurement accuracy. Following ROI extraction,

the fringe density is computed from the selected regions, capturing temporal variations induced by the periodic motion of the shaker. These variations serve as the basis for deriving vibration displacement parameters. Direct frequency analysis of the fringe density signal is often hindered by spectral leakage, particularly in low-frequency, finite-length signals, leading to distorted frequency components and reduced estimation accuracy. To address this, ITCM is introduced, which enhances frequency estimation by dynamically adjusting the time-shift interval and systematically removing statistical outliers from spectral data, thereby improving spectral resolution and robustness. This refinement ensures reliable extraction of vibration parameters under challenging low-frequency conditions. To estimate peak displacement, a *sine approximation method* (SAM) is used to fit the extracted displacement data, enabling precise reconstruction of the vibration waveform and accurate identification of key motion characteristics, including amplitude and phase. This integrated approach ensures robust and accurate measurement of low-frequency vibration parameters.

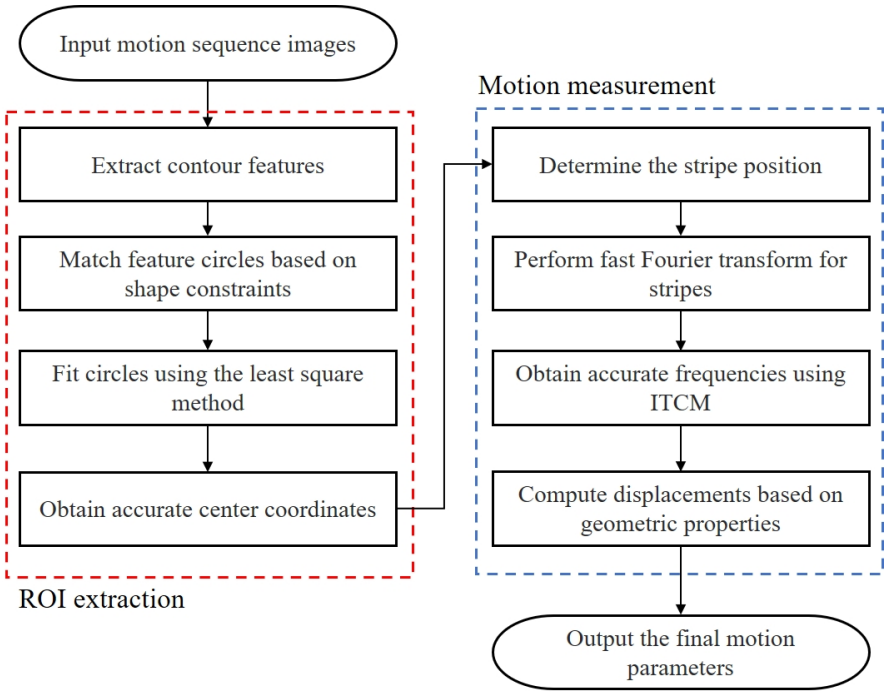

Fig. 1. Overall workflow of the proposed method.

2.1. ROI Extraction

Accurate extraction of ROI is fundamental to reliable fringe pattern analysis as it directly impacts marker localization precision and the quality of subsequent image processing. This study employs a robust ROI determination strategy by utilizing four circular reference markers that geometrically enclose the central fringe region, as depicted in Fig. 2. To ensure stable and consistent localization of the ROI in sequential image frames, even under conditions involving motion-induced deformation or perspective variation, three geometric constraints are applied, including roundness, eccentricity, and convexity [20]:

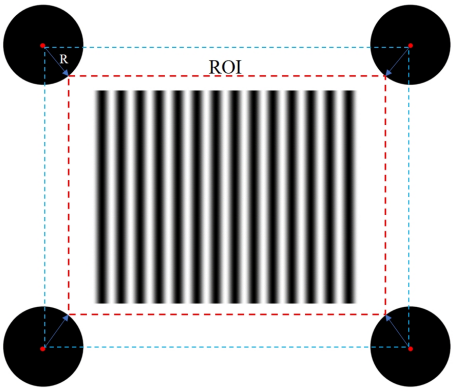

Fig. 2. Diagram of the characterization markers.

1. Roundness C quantifies the circularity of a shape, defined as the ratio of its area A to the square of its perimeter P:

$$C = 4\pi A/P^2, \tag{1}$$

where the value of C approaching 1 indicates high circularity.

2. Eccentricity E measures the deviation from a perfect circle, computed based on image moments:

$$E = \sqrt{1 - b^2/a^2}, \tag{2}$$

where a and b are the lengths of the semi-major and semi-minor axes, respectively, derived from the inertia properties of the shape. Values of E near 0 signify a greater similarity to a circle.

3. Convexity V assesses the extent to which a shape fills its convex hull:

$$V = S/H, \tag{3}$$

where S is the area of the shape and H is the area of its convex hull. A value of V close to 1 indicates minimal concavity and strong conformity to circular geometry.

Contours that meet these criteria are retained and a least-squares circle fitting method is applied to estimate the radius R of each marker. The centroid of each marker is computed using the image moment method, with the general form of the $(i + j)$-order spatial moment given by:

$$m_{ij} = \sum_y \sum_x x^i y^j I(x, y) \tag{4}$$

For centroid determination, only first-order moments are required. The centroid coordinates $(\overline{x}, \overline{y})$ are calculated as follows:

$$\overline{x} = m_{10}/m_{00},\ \overline{y} = m_{01}/m_{00}, \tag{5}$$

where m_{00} is the zero-order moment (total intensity), and m_{10} and m_{01} are the first-order moments along the x- and y-axes, respectively.

The final ROI is defined by forming a quadrilateral bounding box using the four computed centroids. This ensures precise and consistent localization of the fringe region while effectively excluding background interference and non-target features, providing a robust foundation for subsequent fringe density analysis and vibration parameter extraction.

2.2. Measurement Principle

The proposed method for low-frequency vibration measurement relies on analyzing temporal variations in fringe density within captured image sequences. During operation, a low-frequency shaker induces periodic motion in characteristic markers affixed to its surface, moving perpendicularly to the imaging plane relative to the image acquisition system. This motion causes cyclic changes in the distance between the markers and the camera, manifesting themselves as periodic fluctuations of fringe density in the image sequence. Specifically, the fringe density dynamically increases or decreases over time. By extracting and analyzing these density variations, the vibration parameters of the shaker, including frequency and amplitude, can be accurately estimated [21]. The measurement principle is illustrated in Fig. 3.

To quantitatively determine displacement, the proposed method integrates data on fringe density variation with the intrinsic parameters of the camera and the geometrical properties of the fringe marker. Based on the pinhole imaging model, the following relationships are established.

Under static conditions, the actual length L of a central fringe in the marker corresponds proportionally to its image length a on the sensor:

$$L/a = D/F, \tag{6}$$

where D is the object distance and F is the image distance on the sensor plane.

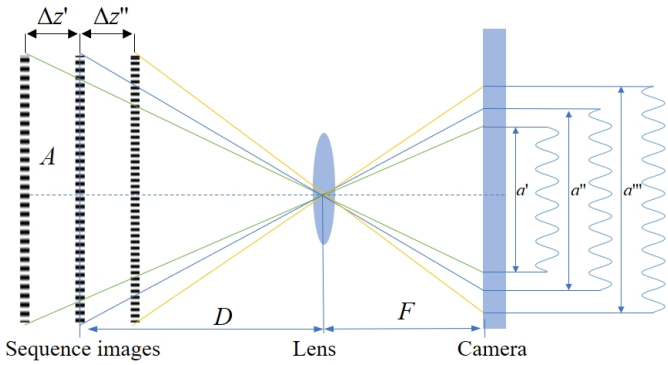

Fig. 3. Principle of fringe-based vibration measurement.

During vibration, the fringe image length a' varies with the change in distance between marker and camera. Therefore, the following expression is obtained under dynamic conditions:

$$(D + \Delta z)/F = L/a', \tag{7}$$

where Δz is the displacement of the vibrating marker relative to the static position.

Since fringe density d is inversely proportional to fringe image length, this expression can be reformulated in terms of fringe density under static d and vibrating d' conditions:

$$\Delta z = D\left(\frac{a'}{a} - 1\right) = D\left(\frac{d}{d'} - 1\right). \tag{8}$$

Finally, the actual physical displacement is derived from the variation in fringe density, enabling an accurate measurement of the motion of the shaker.

2.3. Improved Time-shifting Correction Method

Accurate frequency-domain transformation of sinusoidal fringe signals is essential for extracting vibration parameters in low-frequency displacement measurements. Direct application of a *fast Fourier transform* (FFT) to the fringe density signal often introduces significant errors because of the finite duration of the signal, causing spectral leakage that spreads energy across adjacent spectral bins and distorts frequency components. To address these issues, a *time-shifting correction method* (TCM) is used, which improves frequency estimation by analyzing phase differences between two versions of time-shifted signals [22]. This phase relationship enables correction of the fundamental frequency beyond the resolution limit of discrete FFT. However, conventional TCM, with its fixed time-shift lengths, is sensitive to noise and signal variability, compromising robustness.

To improve stability and reliability, this study proposes the ITCM, which incorporates adaptive time-lapse selection and statistical outlier elimination. The implementation details of both TCM and ITCM are presented below, with the overall workflow of ITCM illustrated in Fig. 4.

The fringe signal is modeled as a discrete-time sinusoidal sequence:

$$x(n) = A_s \cos(2\pi f_0 N T_s + \phi), \tag{9}$$

where A_s is the signal amplitude, f_0 is the true vibration frequency, ϕ is the initial phase, $T_s = 1/f_s$ is the sampling period, f_s is the sampling frequency, N is the discrete time sample index.

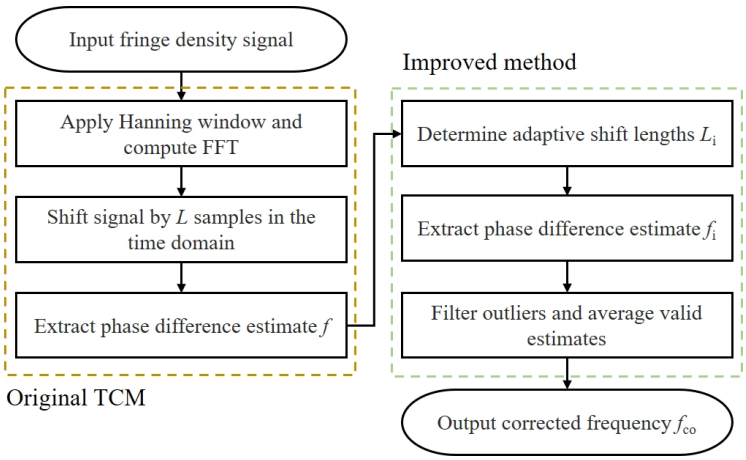

Fig. 4. Workflow of ITCM.

To mitigate spectral leakage due to finite duration of the signal, a Hanning window is applied to the time-domain signal:

$$\omega(n) = 0.5 - 0.5\cos\left(2\pi n/(N-1)\right). \tag{10}$$

For the signal after adding the Hanning window, its *discrete Fourier transform* (DFT) formula is:

$$X_\omega(k) = \sum_{n=0}^{N-1} x_\omega(n) e^{-j\frac{2\pi}{N}kn}, \tag{11}$$

where $X_\omega(k)$ represents the frequency spectrum of the windowed signal.

For further refinement, the signal is temporally shifted by L samples:

$$x_L(n) = x(n + L). \tag{12}$$

According to the Fourier shift theorem, this time-domain shift induces a linear phase shift in the frequency domain:

$$X_L(k) = X(k) \cdot e^{j\frac{2\pi}{N}kL}. \tag{13}$$

The phase shift between the original and shifted signals is computed as:

$$\Delta\theta = \arg(X_L(k)) - \arg(X(k)). \tag{14}$$

The corrected frequency is then:

$$f_{\text{co}} = f_0 + \frac{\Delta\theta \cdot f_s}{2\pi L}, \tag{15}$$

where f_0 is the coarse frequency estimate from the FFT.

ITCM enhances this process by replacing the static time shift L_0 with a dynamic selection strategy, evaluating a set of shift lengths L_i within an adaptive range:

$$L_i = L_0 \pm \lambda N, \tag{16}$$

where λ is an adaptive coefficient adjusted based on the spectral properties of the fringe signal and N is the length of the signal.

The adaptive coefficient λ is computed based on the rate of amplitude variation:

$$\lambda = k_1 \cdot \frac{\sum_{i=1}^{N-1} |x(i) - x(i-1)|}{\sum_{i=1}^{N} |x(i)|} \tag{17}$$

where *x(i)* is the signal amplitude at index I and k_1 is a scaling factor. In practical implementation, the initial shift length L_0 is set proportional to the signal length, typically $N/4$. The scaling factor k_1 is empirically tuned within the range of 0.5 to 1 to balance sensitivity and stability. This adaptive approach ensures that time-shift length L accommodates various vibration conditions, thus enhancing the stability of the correction.

For each time-shift length L_i, a corrected frequency f_i is estimated using the TCM procedure. These estimates undergo statistical filtering based on a confidence threshold, comparing each f_i against the mean of all candidate frequencies:

$$|f_i - \overline{f}_i| \le \varepsilon, \quad \varepsilon = k_2 \cdot \sqrt{\frac{1}{n}\sum_{i=1}^{n}\left(f_i - \overline{f}\right)^2}, \tag{18}$$

where $\overline{f}$ is the mean frequency and ε is the confidence threshold. k_2 is typically 1.96 for a 95% confidence interval, assuming a normal distribution, and n is the number of frequency estimates.

Only frequencies within this interval are retained. The final corrected frequency f_{co} is the average of valid estimates:

$$f_{\text{co}} = \frac{1}{M}\sum_{i=1}^{M} f_i, \tag{19}$$

where M is the number of valid frequency estimates.

By integrating adaptive time-shifting and statistical refinement, ITCM significantly enhances the reliability of frequency estimation, effectively mitigating spectral leakage and signal variability. Moreover, the computational cost of ITCM is primarily dominated by FFT, which exhibits a complexity of $O(N \log N)$, where N is the length of the signal. Additional operations, including temporal shifting, adaptive coefficient evaluation, and outlier elimination, scale linearly with N. Consequently, the overall complexity remains $O(N \log N)$, ensuring computational efficiency. These characteristics make ITCM particularly suitable for real-world low-frequency vibration scenarios characterized by non-ideal and noisy conditions.

2.4. Calculation of Motion Parameters

Using the corrected frequency obtained from ITCM, the actual displacement of the vibrating target is estimated based on a camera model. Leveraging the geometric projection relationship between object space and image space, the out-of-plane displacement Δz relative to the static reference position is computed as:

$$\Delta z = D\left(\frac{d}{d'} - 1\right) = f_c \cdot \left(1 + \frac{L}{p \cdot n}\right) \cdot \left(\frac{d}{d'} - 1\right), \tag{20}$$

where n is the number of pixels that correspond to the fringe under static conditions, p is the pixel size of the camera sensor, and f_c is the focal length of the camera.

This formulation enables precise recovery of displacement over time, with the resulting displacement signal $\Delta z(t)$ exhibiting a quasi-sinusoidal waveform for systems under harmonic excitation.

To enhance accuracy and suppress high-frequency noise, SAM is applied, which fits the extracted displacement signal to a sinusoidal function:

$$\widetilde{z}(t) = A_m \sin(2\pi f_{\mathrm{co}} t + \phi), \tag{21}$$

where A_m is the estimated peak displacement amplitude and f_{co} is the corrected frequency from ITCM. The fitting is performed using nonlinear least squares optimization.

Finally, the acceleration is derived by computing the second-order derivative of the fitted displacement curve. This process completes the extraction of all motion parameters, including displacement, frequency, and acceleration with the proposed measurement method.

3. Experiments and Analysis of Results

To achieve accurate measurement of motion parameters in low-frequency shakers, this study develops a monocular vision-based vibration measurement system. The system architecture, depicted in Fig. 5, comprises three core components: (1) a high-contrast characteristic marker, (2) an image acquisition unit, and (3) a data processing unit.

During operation, a controller drives the shaker to produce vibrational motion at predefined frequencies and amplitudes. Custom-designed fringe markers, securely attached to the shaker's surface, serve as visual references that mirror the dynamic motion of the shaker. A high-resolution camera continuously captures image sequences of the moving fringe patterns. These frames are transmitted to a computer system, where advanced image processing algorithms extract temporal variations in fringe density, a critical indicator of the displacement and frequency characteristics of the shaker. By analyzing these variations using ITCM, the system accurately computes essential vibration parameters, including displacement amplitude, frequency, and acceleration.

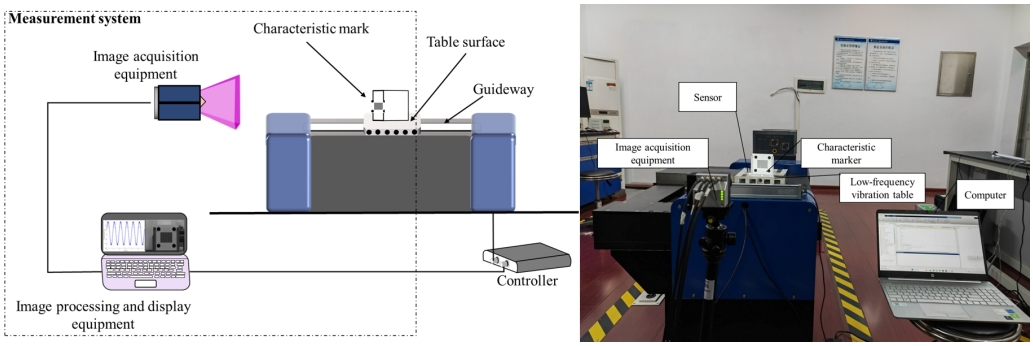

Fig. 5. Schematic diagram and physical prototype for monocular vision-based measuring motion parameters.

The low-frequency shaker used in the experiments is capable of generating sinusoidal excitations with a frequency range of 0.01 Hz to 10 Hz and a maximum displacement amplitude of 250 mm, effectively simulating low-frequency motion scenarios commonly encountered in structural diagnostics and calibration applications. To capture image sequences of the marker's motion during vibration, a high-performance CMOS camera (model: boA5120-150 cm by Basler) with a resolution of 25 megapixels and a pixel size of 2.5 µm × 2.5 µm is employed. This imaging setup is critical for detecting subtle variations in fringe density induced by the shaker motion, which are subsequently analyzed to extract precise displacement and frequency data.

3.1. Robustness Verification

To assess the robustness of ITCM under variable imaging conditions, an experiment is designed in which the marker is kept completely stationary while the illumination level is gradually adjusted from dim to bright, as shown in Fig. 6. This experimental scenario simulates practical conditions where ambient lighting fluctuations or camera exposure adjustments cause significant contrast variations in fringe patterns, potentially compromising the accuracy of frequency-domain processing and fringe density estimation. By conducting measurements in the absence of motion, the experiment isolates illumination as the sole disturbance factor, enabling a direct evaluation for the robustness of each method.

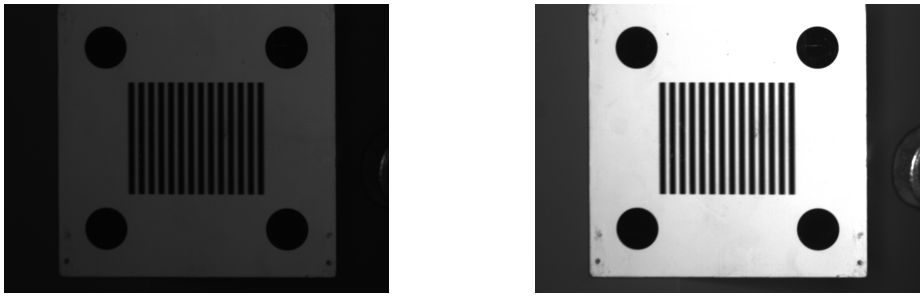

(a) (b)

Fig. 6. Stripe pattern illumination level from dim to bright.

The fringe density signals obtained under different illumination levels are processed using the *energy center correction method* (ECCM), TCM, and ITCM. The comparison results are presented in Fig. 7. As illumination increases from dark to bright conditions, both ECCM and conventional TCM exhibit noticeable fluctuations in the estimated fringe density, particularly under low-contrast conditions where noise interference becomes dominant. In contrast, ITCM consistently maintains a stable estimation accuracy throughout the entire illumination range, with minimal deviation from the expected stationary baseline. These findings demonstrate that ITCM is significantly less sensitive to illumination variations compared to ECCM and TCM, ensuring reliable fringe density extraction even in measurement environments subject to fluctuating brightness or inconsistent imaging quality.

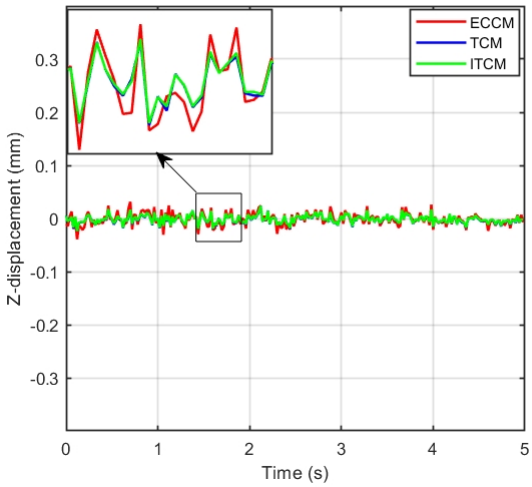

Fig. 7. Comparison of fringe density estimation using ECCM, TCM, and ITCM.

3.2. Measurement of Displacement

To evaluate the accuracy and reliability of the proposed monocular vision-based measurement method, a benchmark comparison is conducted against a traditional sensor-based method. The low-frequency shaker is equipped with an integrated grating ruler displacement sensor, a well-established and high-precision device widely used in industrial and metrological applications. During testing, the shaker is programmed to generate sinusoidal vibrations across a range of frequencies and amplitudes. Identical experimental conditions are applied to both the monocular vision-based system and the grating ruler, ensuring a fair and consistent basis for performance evaluation.

Comparative experiments are conducted over a frequency range from 0.01 Hz to 10 Hz, covering ultra-low- to moderate low-frequency vibration scenarios. The peak displacement values measured with the proposed vision-based method were compared with those obtained from the grating ruler sensor. The results, summarized in Table 1, demonstrate a high degree of consistency between the two methods. Both systems accurately matched the nominal excitation frequencies, with displacement amplitude errors between the vision-based method and the grating ruler remaining within 0.5% across all tested conditions. This result underscores the robustness and accuracy of the proposed method, validating its efficacy as a non-contact alternative for low-frequency displacement measurement.

Table 1. Comparison of displacement and amplitude measurements using the grating ruler and monocular vision.

Given value		Grating ruler		Monocular vision		Error
F (Hz)	Amp (mm)	F (Hz)	Amp (mm)	F (Hz)	Amp (mm)	
0.01	40	0.01	40.1052	0.01	40.0858	0.05%
0.02	40	0.02	39.9887	0.02	39.9467	0.11%
0.05	40	0.05	40.0613	0.05	40.1284	0.17%
0.08	40	0.08	39.9945	0.08	40.0373	0.11%
0.1	40	0.10	40.4904	0.10	40.5326	0.10%
0.2	40	0.20	40.1058	0.20	40.1665	0.15%
0.5	30	0.50	30.1508	0.50	30.1088	0.14%
0.8	19	0.80	19.3661	0.80	19.4062	0.21%
1	15	1.00	15.5277	1.00	15.5423	0.09%
2	8	2.00	8.0874	2.00	8.0833	0.05%
5	3	5.00	2.9965	5.00	3.0013	0.16%
8	1.9	8.00	1.8942	8.00	1.8970	0.15%
10	1.5	10.00	1.4952	10.00	1.5007	0.37%

3.3. Acceleration Measurement

To assess the accuracy and reliability of the proposed monocular vision-based method for measuring motion acceleration, a comparative analysis is conducted against a traditional acceleration sensor under identical experimental conditions. An MSV3100A-10 acceleration sensor, depicted in Fig. 8, is used as the reference device due to its established sensitivity and reliability in low-frequency vibration testing.

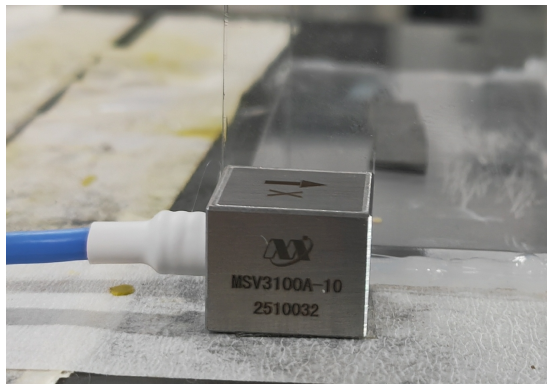

Fig. 8. Diagram of the acceleration sensor used.

The shaker is subjected to sinusoidal excitations identical to those used in the displacement experiments, with both the monocular vision-based method and the reference acceleration sensor recording the resulting motion accelerations across a range of frequencies. The measured acceleration values are presented in Table 2. Both systems exhibited high accuracy in capturing acceleration amplitudes.

Table 2. Comparison of acceleration and THD values using the acceleration sensor and monocular vision.

Acceleration sensor		**Monocular vision**	
Acc (mm/s^2)	**THD**	**Acc (mm/s^2)**	**THD**
16.122	16.908	16.066	0.003
64.594	5.535	63.683	0.005
304.047	2.382	298.356	0.006
499.642	0.858	492.290	0.004
626.177	1.152	616.048	0.005
1304.296	0.800	1295.558	0.004
3021.477	0.756	3054.106	0.004
4894.618	0.645	4812.144	0.010
6039.429	0.486	5971.113	0.011

The *total harmonic distortion* (THD) values are calculated to evaluate the quality of the acceleration signals, since THD indicates the purity of the signal by measuring the extent of unwanted harmonic distortions relative to the fundamental frequency. The results show that the monocular vision-based method consistently achieves significantly lower THD values compared to the traditional acceleration sensor, indicating its ability to capture cleaner and less distorted acceleration waveforms. This advantage is particularly pronounced in low-frequency excitations, where conventional sensors are prone to mechanical coupling effects and signal degradation.

The enhanced signal fidelity of the vision-based system stems from its non-contact measurement principle and high spatial resolution, which minimize susceptibility to external noise, vibration-induced artifacts, and mechanical interference. These characteristics make the proposed method highly suitable for applications that require high-precision, low-noise acceleration measurements, such as structural health monitoring, sensor calibration, and dynamic system diagnostics.

3.4. Displacement Curve

To verify the accuracy of the proposed method in measuring displacement waveforms, a monocular vision-based approach was used to record the displacement responses of the object under several selected excitation frequencies. The displacement curves measured using the proposed method under low-frequency sinusoidal excitation are presented in Fig. 9. The results demonstrate smooth and periodic sinusoidal waveforms that closely align with the expected motion profiles. The near absence of waveform distortion highlights the capability of the proposed method to accurately capture dynamic displacement characteristics, even at very low frequencies where traditional systems often face challenges due to noise or resolution limitations.

The aforementioned findings highlight the robustness of the proposed method in practical testing environments, confirming its suitability for applications requiring precise and high-fidelity displacement measurements in low-frequency vibration scenarios.

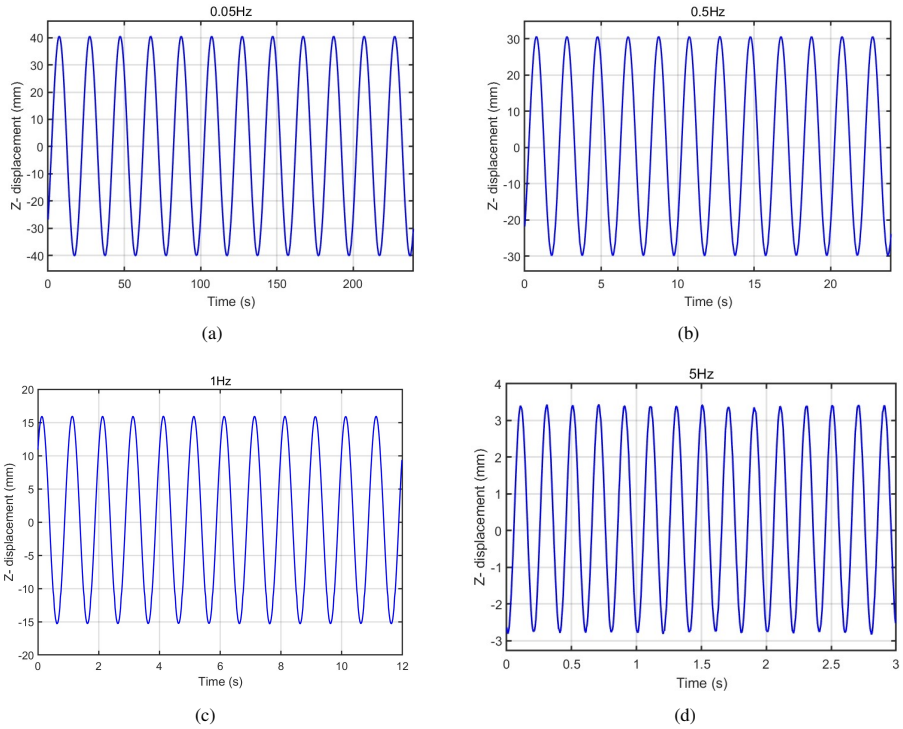

Fig. 9. Displacement measurement curves at different frequencies using the proposed method.

4. Conclusions and Future Work

This study introduces a novel non-contact vibration measurement method for low-frequency shakers, leveraging monocular vision to analyze fringe density variations from high-contrast characteristic markers. The proposed method accurately extracts critical vibration parameters, including frequency, displacement amplitude, and acceleration. An improved time-shifting correction method is developed to enhance frequency estimation precision through adaptive time-lapse adjustments and statistical outlier elimination. The experimental results validate the high accuracy of the proposed method, achieving displacement errors within 0.5% and lower total harmonic distortion in acceleration measurements, particularly at frequencies below 1 Hz. The proposed solution also demonstrates robust stability, surpassing traditional acceleration sensors in low-frequency scenarios. Future work will explore extending the proposed method to multi-axis vibration analysis and its application in fields, such as structural health monitoring, non-destructive testing, and precision equipment diagnostics.

Acknowledgements

This work was supported by the Chinese National Key Research and Development Programme under Grant No. 2022YFF0609400, Postgraduate Research Fund of Guizhou Province under Grant Nos. 2024YJSKYJJ094 and 2024YJSKYJJ095 and Project of the Natural Science Foundation of Hunan Province Nos. 2022JJ90036 and 2024JJ8307.

References

[1] Cui, G., Li, B., Tian, W., Liao, W., & Zhao, W. (2021). Dynamic modeling and vibration prediction of an industrial robot in manufacturing. *Applied Mathematical Modelling*, *105*, 114–136. https://doi.org/10.1016/j.apm.2021.12.031

[2] Villarroel, A., Zurita, G., & Velarde, R. (2019). Development of a low-cost vibration measurement system for industrial applications. *Machines*, *7*(1), 12. https://doi.org/10.3390/machines7010012

[3] Zhong, J., Liu, D., Chi, S., Tu, Z., & Zhong, S. (2022). Vision-based fringe projection measurement system for radial vibration monitoring of rotating shafts. *Mechanical Systems and Signal Processing*, *181*, 109467. https://doi.org/10.1016/j.ymssp.2022.109467

[4] Yang, M., Liu, Z., Cai, C., Wang, Y., Yang, J., & Yang, J. (2021). Monocular vision-based calibration method for the axial and transverse sensitivities of low-frequency triaxial vibration sensors with the elliptical orbit excitation. *IEEE Transactions on Industrial Electronics*, *69*(12), 13763–13772. https://doi.org/10.1109/tie.2021.3130325

[5] Yang, M., Zhang, J., Cai, C., Wang, Y., Liu, Z., & Wang, D. (2023). A superefficient monocular vision dynamic calibration method used for determining the sensitivities of low-frequency linear and vibration angular sensors. *IEEE Transactions on Industrial Electronics*, *71*(9), 11716–11720. https://doi.org/10.1109/tie.2023.3337540

[6] Fu, Y. (2009). Low-frequency vibration measurement by temporal analysis of projected fringe patterns. *Optics and Lasers in Engineering*, *48*(2), 226–234. https://doi.org/10.1016/j.optlaseng.2009.03.003

[7] Ding, J., Wang, Y., Wang, M., Sun, Y., Peng, Y., Luo, J., & Pu, H. (2022). An active geophone with an adjustable electromagnetic negative stiffness for low-frequency vibration measurement. *Mechanical Systems and Signal Processing*, *178*, 109207. https://doi.org/10.1016/j.ymssp.2022.109207

[8] Wu, Q., Yang, M., Liu, Z., Cai, C., Wang, Y., & Wang, D. (2024). Monocular vision-based decoupling measurement method for multi-degree-of-freedom motion. *IEEE Sensors Journal*, *24*(21), 35092–35100. https://doi.org/10.1109/jsen.2024.3457627

[9] Li, L., Ohkubo, T., & Matsumoto, S. (2020). Vibration measurement of a steel building with viscoelastic dampers using acceleration sensors. *Measurement*, *171*, 108807. https://doi.org/10.1016/j.measurement.2020.108807

[10] Link, A., Täubner, A., Wabinski, W., Bruns, T., & Elster, C. (2006). Calibration of accelerometers: determination of amplitude and phase response upon shock excitation. *Measurement Science and Technology*, *17*(7), 1888–1894. https://doi.org/10.1088/0957-0233/17/7/030

[11] Lin, J., Guan, J., Wen, F., & Tan, J. (2017). High-resolution and wide range displacement measurement based on planar grating. *Optics Communications*, *404*, 132–138. https://doi.org/10.1016/j.optcom.2017.03.012

[12] Garg, N., & Schiefer, M. (2017). Low frequency accelerometer calibration using an optical encoder sensor. *Measurement*, *111*, 226–233. https://doi.org/10.1016/j.measurement.2017.07.031

[13] Li, Q., Wang, S., Guan, B., & Wang, G. (2007). A machine vision method for the measurement of vibration amplitude. *Measurement Science and Technology*, *18*(5), 1477–1486. https://doi.org/10.1088/0957-0233/18/5/038

[14] Tang, W., Tian, L., & Zhao, X. (2016). Research on displacement measurement of disk vibration based on machine vision technique. *Optik*, *127*(8), 4173–4177. https://doi.org/10.1016/j.ijleo.2016.01.019

[15] Dong, C., Ye, X., & Jin, T. (2017). Identification of structural dynamic characteristics based on machine vision technology. *Measurement*, *126*, 405–416. https://doi.org/10.1016/j.measurement.2017.09.043

[16] Zhong, J., Zhong, S., Zhang, Q., Liu, S., Peng, Z., & Maia, N. (2018). Real-time three-dimensional vibration monitoring of rotating shafts using constant-density sinusoidal fringe pattern as tri-axial sensor. *Mechanical Systems and Signal Processing*, *115*, 132–146. https://doi.org/10.1016/j.ymssp.2018.05.049

[17] Yang, M., Cai, C., Liu, Z., & Wang, Y. (2020). Monocular vision-based calibration method for determining frequency characteristics of low-frequency vibration sensors. *IEEE Sensors Journal*, *21*(4), 4377–4384. https://doi.org/10.1109/jsen.2020.3035581

[18] Zuo, S., Cai, C., Yang, M., Liu, Z., Wang, D., & Wang, Y. (2023). Prior information-based motion blur image restoration method for the low-frequency sinusoidal vibration measurements with machine vision. *Signal Processing*, *212*, 109132. https://doi.org/10.1016/j.sigpro.2023.109132

[19] Zhong, J., Zhong, S., Zhang, Q., Zhuang, Y., Lu, H., & Fu, X. (2016). Vision-based measurement system for structural vibration monitoring using non-projection quasi-interferogram fringe density enhanced by spectrum correction method. *Measurement Science and Technology*, *28*(1), 015903. https://doi.org/10.1088/1361-6501/28/1/015903

[20] Chen, M. (2002). Roundness measurements for discontinuous perimeters via machine visions. *Computers in Industry*, *47*(2), 185–197. https://doi.org/10.1016/s0166-3615(01)00143-9

[21] Zhong, S., Zhong, J., Zhang, Q., & Maia, N. (2017). Quasi-optical coherence vibration tomography technique for damage detection in beam-like structures based on auxiliary mass induced frequency shift. *Mechanical Systems and Signal Processing*, *93*, 241–254. https://doi.org/10.1016/j.ymssp.2017.02.005

[22] Kang, D., Jiang-Kai, L., & Ming, X. (2002). Time-shifting correcting method of phase difference on discrete spectrum. *Applied Mathematics and Mechanics*, *23*(7), 819–827. https://doi.org/10.1007/bf02456978

Yunpeng Wang received his B.Eng. degree from the College of Electrical and Information Engineering in Hunan University of Technology, Hunan, China, in 2023. He is currently pursuing his M.Sc. degree in the Electrical Engineering College of Guizhou University, Guiyang, China. His current research interests include machine vision detection and vibration monitoring.

Kui Gan received his B.Eng. degree in computer science and technology from Central South University, China, in 2009. He is currently a senior engineer affiliated with the Institute of Mechanics and Acoustics Metrology at the Hunan Institute of Metrology and Testing (Changsha, China), where his research focuses on force measurement, torque, rotational speed, and vibration metrology technologies and applications.

Xiongheng Cao is currently a senior engineer at the Hunan Institute of Metrology and Testing. He holds an M.Sc. degree from National University of Defense Technology. His main research interests are acoustics and vibration metrology.

Shanshan Wu received her B.Eng. degree in transportation civil engineering from Changsha University of Science and Technology in 2012. Currently, she works as a calibrator at the Institute of Mechanical and Acoustic Metrology Science of the Hunan Institute of Metrology and Testing, with a research focus on mechanical and acoustic metrology.

Hongjiang Chen received his Ph.D. degree from the School of Resources and Safety Engineering, Central South University, in 2010. He is currently a distinguished professor with the Department of Force and Acoustic Metrology at the Hunan Institute of Metrology and Testing in Changsha, China. His research interests include laser and machine vision detection as well as vibration metrology and monitoring.

Deguang Wang received his B.Sc. degree in automation and his Ph.D. degree in control science and engineering from Xidian University, Xi'an, China, in 2014 and 2019, respectively. From 2016 to 2017, he was a visiting Ph.D. student with the Systems Control Group, Department of Electrical and Computer Engineering, University of Toronto, Canada. He is currently a lecturer with Guizhou University, Guiyang, China. His current research interests include supervisory control theory, fault diagnosis, and swarm intelligence algorithms.